Transport and magnetic properties of $RERuSn_3$ (RE=La, Ce, Pr, Nd, Sm): a heavy fermion compound $CeRuSn_3$ and a new valence fluctuating compound $SmRuSn_3$

1991 J. Phys.: Condens. Matter 3 8917

(http://iopscience.iop.org/0953-8984/3/45/014)

J. Phys.: Condens. Matter 3 (1991) 8917–8929. Printed in the UK

Transport and magnetic properties of $RERuSn_3$ (RE = La, Ce, Pr, Nd, Sm): a heavy fermion compound $CeRuSn_3$ and a new valence fluctuating compound $SmRuSn_3$

T Fukuhara†, I Sakamoto‡ and H Sato
Department of Physics, Tokyo Metropolitan University Minami-Ohsawa 1-1, Hachioji-shi, Tokyo 192-03, Japan

Received 4 October 1990, in final form 22 July 1991

Abstract. The electrical resistivity, thermoelectric power, Hall effect, magnetoresistivity, magnetic susceptibility and magnetization of intermetallic ternary compounds $RERuSn_3$ (RE = La, Ce, Pr, Nd and Sm), $CeRuSn_x$ ($2.85 \leq x \leq 3.15$), $CeRu(Sn_{1-y}In_y)_3$ and $NdRuSn_{2.91}$ have been measured. $CeRuSn_3$ was reported to be a heavy fermion compound with an enormous coefficient of electronic specific heat $\gamma = 1.67\ J\ K^{-2}$/mole at 0.6 K. In order to gain a deeper insight into the heavy fermion state of $CeRuSn_3$, non-stoichiometric compounds $CeRuSn_x$ ($2.85 \leq x \leq 3.15$) have also been investigated. The low temperature resistivity shows a maximum at $x = 3.0$ as a function of x. Sn deficient samples show three step phase transitions at 33 K, 4 K and 1.3 K. $PrRuSn_3$ and $NdRuSn_3$ do not show any magnetic ordering down to 1.8 K. $SmRuSn_3$ is a new valence fluctuating compound with an antiferromagnetic ordering at 6 K.

1. Introduction

Rare-earth (RE) intermetallic compounds show a wide variety of magnetic behaviour depending on the kind of RE ions.

In Ce compounds, hybridization of the 4f-electron state with the ligand state plays an important role in their magnetic properties. The hybridization causes a Kondo effect at Ce-ion sites, while the intersite exchange RKKY interaction brings about some magnetic order. The ground state of Ce compounds is basically determined by the relative strength of the Kondo effect and the RKKY interaction. Several Ce intermetallics such as $CeCu_6$ [1] or $CeAl_3$ [2], exhibit no long range magnetic order down to the mK region. At the lowest temperatures, 4f electrons in these compounds are delocalised and become band electrons which have a large effective mass. This effect arises from a complex many body effect which has not been completely solved.

In Pr compounds, where the Pr^{3+} ion is the non-Kramers type, the ratio of the RKKY interaction to the crystal field splitting width between the ground singlet state and the excited state determines whether the system has a magnetic transition or not. For

† Present address: Toyama Prefectural University, Kosugi-mati, Toyama 939-03, Japan.
‡ Present address: Nagoya Institute of Technology, Nagoya-Shi, Aichi 466, Japan.

0953-8984/91/458917 + 13 $03.50

example, $PrCu_6$ shows no magnetic order due to 4f electrons [3], while PrB_6 orders antiferromagnetically below 7 K [4].

Nd compounds usually exhibit a magnetic ordering of localized moments. A number of Nd compounds have very complex and interesting magnetic structures. For example, $NdCu_6$ is a metamagnetic substance with four discontinuous steps in the magnetization curve [5].

In the Sm^{3+} ion, the first excited state of the spin–orbit coupling multiplet $^6H_{7/2}$ is not so far from the ground state $^6H_{5/2}$ and we cannot ignore thermal excitation of 4f electrons to the excited state. The paramagnetic susceptibility due to Sm^{3+} ions does not obey the Curie–Weiss law. Several Sm compounds exhibit the valence fluctuation phenomenon between the trivalent and divalent Sm states. As a result of such a mixing effect, anomalous magnetic properties appear. For example, $SmSn_3$ [6] is reported to exhibit the dense Kondo behaviour. Only a few valence fluctuating Sm compounds have been reported, while a large number of Ce compounds exhibiting an anomalous mixing effect have been reported.

In order to study the anomalous magnetism of RE intermetallic compounds, it is fruitful to investigate a series of isostructural RE compounds.

The existence of intermetallic compounds with the formula $RERuSn_3$ (RE = La, Ce, Pr, Nd) was reported by Eisenmann and Schäfer [7]. $RERuSn_3$ crystallizes in a cubic structure. $RERuSn_3$ and $RE_3Rh_4Sn_{13}$ [8] are isomorphous compounds with a cubic $Pr_3Rh_4Sn_{13}$ structure. The difference between the two structures is in the occupation of the 2a position in the $Pm\bar{3}n$ space group. The 2a position is occupied by the RE ion in $RERuSn_3$, while in $RE_3Rh_4Sn_{13}$ it is occupied by the Sn ion. These structures have a large RE ion spacing of about 4.9 Å. In the course of this study, we have succeeded in making $SmRuSn_3$ with the same crystal structure.

In this paper, we report on the transport and magnetic properties of the $RERuSn_3$ (RE = La, Ce, Pr, Nd and Sm). For these compounds, we have reported only briefly on the anomalous magnetic properties of $CeRuSn_3$ [9]. In section 2, we describe the sample preparation and the experimental techniques. In section 3.1, we give first an overview of the experimental results on the $RERuSn_3$ system together with brief discussions. The experimental results for $CeRuSn_x$ ($2.85 \leq x \leq 3.15$), $CeRu(Sn_{1-y}In_y)_3$ ($y = 0.15$ and 0.15) and $NdRuSn_{2.91}$ are presented in section 3.2. Finally in section 4, the results are summarized.

2. Experiment

The polycrystalline $RERuSn_3$, $CeRuSn_x$, $NdRuSn_x$ and $CeRu(Sn_{1-y}In_y)_3$ samples were prepared by arc-melting appropriate amounts of the high-purity elements (RE 99.9%, Ru 99.98%, Sn 99.999%) on a water cooled copper hearth. The ingots were wrapped in Ta and Zr foils and were annealed at 950 °C for 3 days in evacuated quartz tubes. In [8], single crystals of intermetallic stannides with the $Pr_3Rh_4Sn_{13}$ structure had been prepared by the molten tin solution method. In the present work, we grew single crystals of a suitable size for the transport measurements by the Czochralski pulling method using a SELEC tri-arc furnace [10].

The samples obtained were analysed by Cu Kα x-ray powder diffraction. No parasitic phase was detected in stoichiometric $RERuSn_3$ and $CeRu(Sn_{1-y}In_y)_3$ ($y = 0.05$ and 0.15), while diffraction patterns of $CeRuSn_x$ ($x \neq 3$) and $NdRuSn_{2.91}$ indicate very weak additional reflections. We have not yet identified the impurity phase the amount of

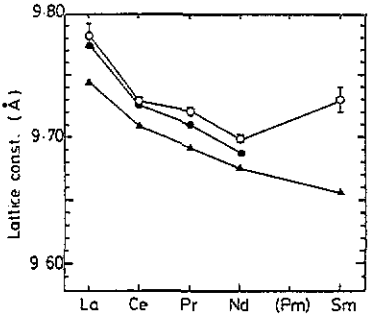

Figure 1. ○, lattice constant of $RERuSn_3$ together with those reported earlier for: ●, $RERuSn_3$ [7]; and ▲, isostructural compound $RERh_xSn_y$ (Remeika *et al* 1980 [8]).

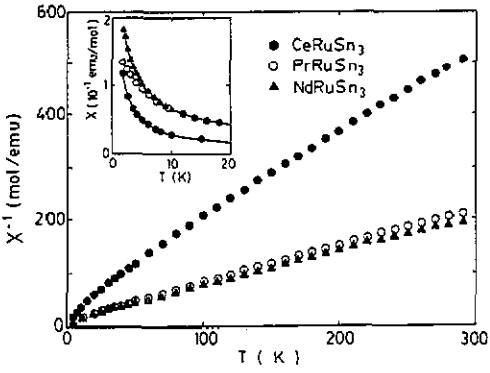

Figure 2. Temperature dependence of reciprocal magnetic susceptibility for $RERuSn_3$ (RE = Ce, Pr and Nd). The inset shows magnetic susceptibility below 20 K.

which, estimated from the intensity of additional lines, is at most several percent. Lattice constants of $RERuSn_3$ were determined from the room temperature powder diffraction pattern of crushed single crystalline samples, using high purity Si powder as an internal standard.

In order to check the ideal composition further, we grew a crystal of $Ce_3Ru_4Sn_{13}$. The x-ray diffraction patterns always showed clear evidence of a considerable amount of Ru_3Sn_7 impurity phase, even if heat treated at several different temperatures, suggesting that $Ce_3Ru_4Sn_{13}$ is not the ideal composition. This fact agrees with the result of the chemical analysis in [7] and supports $RERuSn_3$ as the more stable composition than 3:4:13 in the case of the Ru compound, though we still have some uncertainty for the site occupation.

Single crystal samples for the transport and magnetic measurements were cut into rectangular rods by a spark cutter after being oriented by x-ray Laue diffraction. Typical dimensions of the samples are 1 mm × 1 mm × 5 mm with their longitudinal direction parallel to the [100]. The magnetization and magnetic susceptibility of $RERuSn_3$ were measured up to 55 kOe by the Quantum Design SQUID magnetometer between 1.8 K and 300 K. The electrical resistivity was measured by the standard four-probe method. The thermoelectric power (TEP) was measured by a conventional differential method with a thin copper wire as a reference. The Hall coefficient at 10 kOe was measured by a conventional DC four-probe method or DC five-probe valence method. The high field magnetoresistivity and the Hall resistivity were measured up to 75 kOe.

3. Results and discussion

3.1. $RERuSn_3$ (RE = La, Ce, Pr, Nd and Sm)

Figure 1 shows the lattice constant of $RERuSn_3$ determined by x-ray analysis together with those reported earlier for $RERuSn_3$ [7] and isostructural compounds $RERh_xSn_y$ [9]. The lattice constants of our samples grown by the tri-arc Czochralski method are in

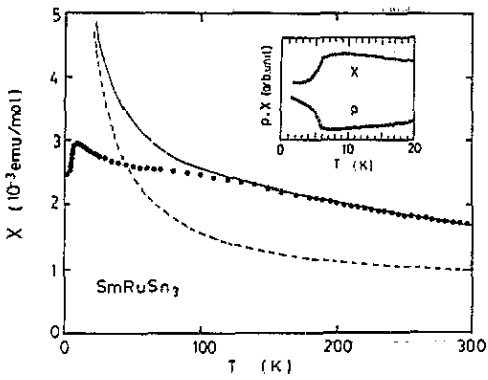

Figure 3. Temperature dependence of magnetic susceptibility for $SmRuSn_3$. The broken curve shows the theoretical susceptibility of Van Vleck–Frank Sm^{3+}. The solid curve shows calculated susceptibility simply assuming $\chi = [(1-a)\chi^{3+} + a\chi^{2+}]$ with $a = 0.2$. The inset shows an enlarged view of magnetic susceptibility and electrical resistivity near the magnetic transition.

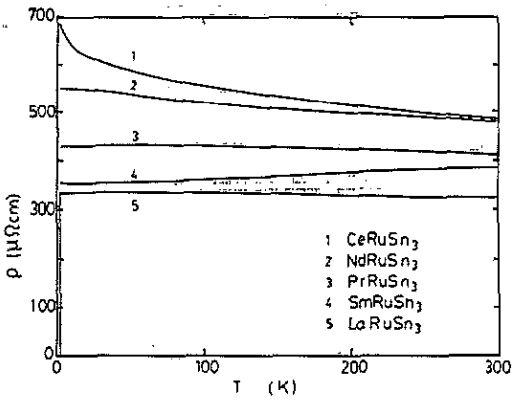

Figure 4. Temperature dependence of electrical resistivity for $RERuSn_3$ (RE = La, Ce, Pr, Nd and Sm)

good agreement with those reported in [7]. The lattice constants of the $RERuSn_3$ system show an anomalous expansion at $SmRuSn_3$, while those for the $RERh_xSn_y$ system exhibit smooth lanthanoid contraction. The expansion for $SmRuSn_3$ suggests the valence fluctuating character of this element.

Figure 2 shows the temperature dependence of the reciprocal magnetic susceptibility for $RERuSn_3$ (RE = Ce, Pr and Nd) between 1.8 K and 300 K. The susceptibility of all the three compounds follows the Curie–Weiss law between 100 K and 300 K. The paramagnetic Curie temperatures are −66 K, −39 K and −31 K and the effective moments are 2.4, 3.5 and 3.6 μ_B/RE atom for RE = Ce, Pr and Nd, respectively. The effective moment of each compound is close to the value for the tri-valent ion (Ce^{3+}:2.56μ_B, Pr^{3+}:3.62μ_B and Nd^{3+}:3.68μ_B). The departure from the Curie–Weiss law below 100 K in each compound is probably due to the crystal field effect.

The inset of figure 2 shows the magnetic susceptibility below 20 K. For all the three systems, no sign of magnetic ordering was observed down to 1.8 K. The susceptibility of $CeRuSn_3$ and $NdRuSn_3$ continues to increase strongly with decreasing temperature down to 1.8 K, which suggests some enhancement of magnetic correlation among 4f electrons at low temperature. Actually in our recent low temperature AC susceptibility measurements [11], $CeRuSn_3$ exhibits some magnetic ordering at 0.6 K. Compared to the other two compounds, the increase of the susceptibility of $PrRuSn_3$ at low temperatures is slightly weaker. This is possibly due to the gradual freezing out of the singlet ground state.

Figure 3 shows the temperature dependence of the magnetic susceptibility for $SmRuSn_3$ between 1.8 K and 300 K. In the figure the broken curve shows the theoretical susceptibility of Van Vleck–Frank Sm^{3+} [12]. The observed susceptibility does not follow the theoretical model. We calculated a susceptibility in a valence fluctuating state χ_{vf} by simply assuming

$$\chi_{vf} = (1-a)\cdot\chi_{3+} + a\cdot\chi_{2+} \qquad (1)$$

where χ_{3+} and χ_{2+} are the susceptibilities of Sm^{3+} and Sm^{2+} respectively. The full curve,

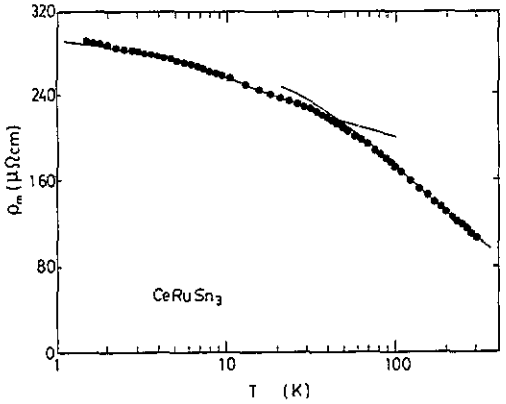

Figure 5. Temperature dependence of the magnetic resistivity for $CeRuSn_3$. The broken curves are the best fitted curves to the Hamman–Fisher law with $T_K = 20$ K and $T_K^h = 120$ K.

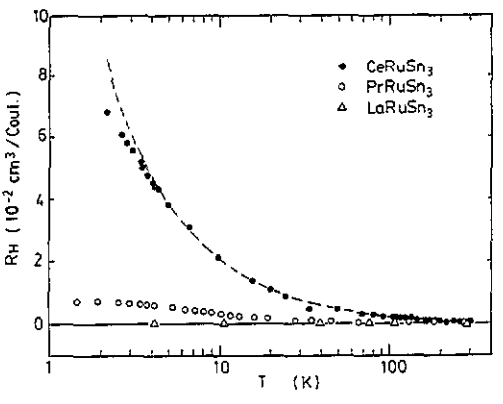

Figure 6. Temperature dependence of the Hall coefficient for $RERuSn_3$ (RE = La, Ce and Pr) at 10 kOe. The broken curve is best fitted to equation (3).

which represents the calculated susceptibility for $a = 0.2$, fits the experimental data near room temperature well. This fact also suggests that the Sm ion is in the valence fluctuating state in $SmRuSn_3$. The observed susceptibility deviates from the calculated value below 150 K and exhibits a broad bump around 100 K. A similar bump was reported for SmB_6 [13] which is a typical valence fluctuating Sm compound.

The inset of figure 3 shows an enlarged view of the magnetic susceptibility and the electrical resistivity near the magnetic transition. The susceptibility shows a broad maximum around 9 K and a drastic decrease at 6 K reflecting the transition into the antiferromagnetic state. The resistivity increase below 6 K implies the formation of an antiferromagnetic gap, which is consistent with the susceptibility results.

Figure 4 shows the temperature dependence of the electrical resistivity for single crystal $RERuSn_3$ between 1.3 K and 300 K. The superconducting transition at 1.5 K for $LaRuSn_3$ has been already reported in [8]. The resistivity at 300 K of $RERuSn_3$ (RE = La, Ce, Pr, Nd and Sm) is 320 ± 30, 490 ± 50, 410 ± 40, 480 ± 50 and 400 ± 40 $\mu\Omega$ cm, respectively. Except for $SmRuSn_3$, the resistivity of single crystal $RERuSn_3$ increases with decreasing temperature near room temperature. Only the resistivity of $SmRuSn_3$ decreases smoothly with decreasing temperature. The resistivity of $LaRuSn_3$ and $PrRuSn_3$ reaches a broad maximum and then decreases slightly at lower temperatures, while the resistivity of $CeRuSn_3$ and $NdRuSn_3$ continues to increase down to 1.3 K. Recently Vodop'yanov *et al* [14] reported a similar temperature dependence of resistivity for $LuRh_{1.2}Sn_4$ which is related to the localization effect due to random occupation of crystal sites by different type of atoms.

Figure 5 shows the magnetic resistivity ρ_m ($\rho_m = \rho_{CeRuSn_3} - \rho_{LaRuSn_3}$) of $CeRuSn_3$. It would seem that coherence effects are totally lacking in this material leaving a pure single ion Kondo dependence due to the large magnitude of the resistivity. We cannot exclude the possibility that the random site occupation contributes to, or even produces, the destruction of coherence. In the figure, we observed two well defined successive logarithmic regimes. This temperature dependence of resistivity is very similar to those for Ce diluted in La compounds such as $La_{1-x}Ce_xCu_6$ [1] or $La_{1-x}Ce_xInCu_2$ [15]. This

behaviour is attributable to the fact that the upper crystal field split levels also contribute to the Kondo effect at high temperature; the Kondo temperature depends on the degeneracy of the f-orbital (N_f). The resistivity in each logarithmic regime is expected to fit the resistivity of a dilute Kondo system as a function of T_K^h and T_K respectively, where T_K^h is the Kondo temperature at higher temperatures ($N_f = 6$) and T_K is that at lower temperatures ($N_f = 2$). The resistivity of a dilute Kondo system is generally well described by the Hamman–Fisher law [16]

$$\rho_m = A + B/2[1 - \ln(T/T^*)/[\ln^2(T/T^*) + \pi^2 S(S+1)]^{1/2}] \qquad (2)$$

where T^* is the Kondo temperature. $A = \rho_u \sin^2 \delta$ and $B = \rho_u \cos^2 \delta$ where ρ_u is the unitarity limit resistivity and δ is the phase shift. In the figure, two solid curves were calculated with $T_K = 20$ K and $T_K^h = 120$ K for a single value $\rho_u = 310\ \mu\Omega$ cm and $S = \frac{1}{2}$. The calculated value of ρ_m fits the experimental data in each temperature range. However, these results are only a rough estimation for lack of information about the crystal field split levels.

Figure 6 shows the temperature dependence of the Hall coefficient for $LaRuSn_3$, $CeRuSn_3$ and $PrRuSn_3$. The Hall coefficient of $LaRuSn_3$ is 2×10^{-4} cm^3/C at 300 K and is weakly temperature dependent. The estimated carrier density based on a single carrier model is 3×10^{16} electrons cm^{-3} at 300 K. The Hall coefficient of $PrRuSn_3$ is 2×10^{-4} cm^3/C at 300 K and gradually increases with decreasing temperature. The increase is attributable to the anomalous Hall effect proportional to the magnetic susceptibility. The Hall coefficient of $CeRuSn_3$ (5×10^{-4} cm^3/C at 300 K) increases monotonically with decreasing temperature to be 6.8×10^{-2} cm^3/C at 4 K. This value is extremely large compared to ordinary heavy fermion compounds. The Hall coefficient of the impurity Kondo system calculated by Fert *et al* [17] on the basis of the skew scattering by Ce impurities is given as

$$R_H = R_0 + \gamma \rho_m \tilde{\chi} \qquad (3)$$

where R_0 is a normal Hall coefficient, $\gamma = -(15/7) g \mu_B k_B^{-1} \cos \delta \sin \delta$, ρ_m is the magnetic resistivity and $\tilde{\chi}$ is the normalized susceptibility. In the figure, the broken curve was calculated from equation (3). In order to estimate the parameters R_0 and γ, we have plotted R_H against $\rho_m \chi$ for $CeRuSn_3$ as shown in the inset of figure 13. The Hall coefficient can be fitted well by the calculated curve down to 4 K, which suggests the dominance of dilute Kondo scattering consistent with the resistivity analysis.

Figure 7 shows the temperature dependence of TEP for $RERuSn_3$ (Re = La, Ce, Pr, Nd and Sm). The TEP of $LaRuSn_3$ at 300 K is positive and decreases monotonically with decreasing temperature without change of sign down to T_c. The TEP of $NdRuSn_3$ is very close to that for $LaRuSn_3$ except for a broad shoulder around 15 K. The TEP of $CeRuSn_3$ has a negative sharp minimum around 6 K and a positive broad maximum around 80 K. In dilute Kondo systems, we generally observe a maximum or a minimum around T_K, so that we can expect that the temperature gives a rough estimation of the Kondo temperature of this system. The temperature 6 K is not so far from 20 K estimated from the temperature dependence of resistivity. The TEP of $PrRuSn_3$ at 300 K is positive and decreases with decreasing temperature. At lower temperatures the TEP has some structures below 20 K, where no appreciable structures have been observed in the resistivity and the magnetic susceptibility. A possible explanation only for the lower temperature TEP structure is the conduction electron scattering accompanying crystal field excitation [18], since we cannot expect to observe the phonon drag effect in such a large residual resistivity sample. The TEP of $SmRuSn_3$ shows a large positive maximum

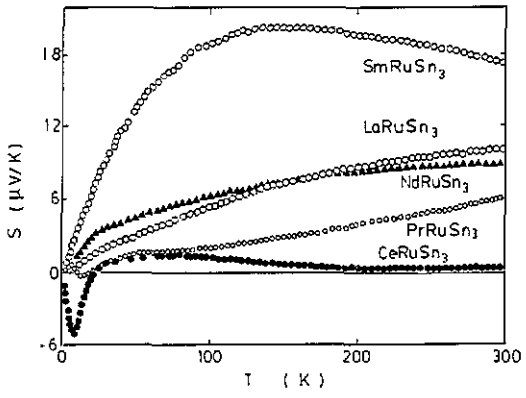

Figure 7. Temperature dependence of the thermoelectric power (TEP) for RERuSn$_3$ (RE = La, Ce, Pr, Nd and Sm).

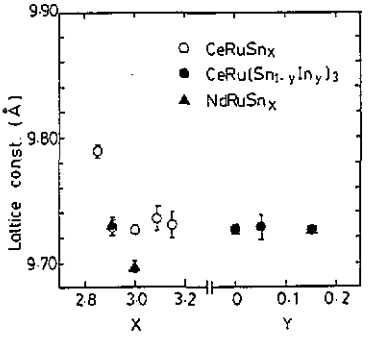

Figure 8. Lattice constant of the series of the non-stoichiometric compounds CeRuSn$_x$ ($2.85 \leqslant x \leqslant 3.15$) and NdRuSn$_x$ ($x = 2.91$ and 3.0) and In alloy CeRu(Sn$_{1-y}$In$_y$)$_3$ ($y = 0.15$ and 0.05).

of $20\mu V\ K^{-1}$ near 150 K. No change of sign is observed down to 1.5 K. This behaviour is similar to the TEP of valence fluctuating compounds such as $CeSn_3$ [19]. The TEP has a small kink corresponding to a magnetic phase transition at 6 K.

3.2. CeRuSn$_x$ ($2.85 \leqslant x \leqslant 3.15$)

As shown in section 3.1, $CeRuSn_3$ does not show any coherence effect. In order to investigate the reasons, we have prepared intentionally off-stoichiometric samples of CeRuSn$_x$ ($2.85 \leqslant x \leqslant 3.15$).

Figure 8 shows the lattice constants of CeRuSn$_x$ ($2.85 \leqslant x \leqslant 3.15$), CeRu(Sn$_{1-y}In_y$)$_3$ ($y = 0.05$ and 0.15) and NdRuSn$_x$ ($x = 3.0$ and 2.91) determined from x-ray powder diffraction measurement. The lattice constant of CeRuSn$_x$ ($2.91 \leqslant x \leqslant 3.15$) is independent of x within experimental error, while the lattice constants of $CeRuSn_{2.85}$ and $NdRuSn_{2.91}$ show some expansion. The lattice constant of CeRu(Sn$_{1-y}$In$_y$)$_3$ ($y = 0.05$ and 0.5) is also independent of y within experimental error.

Figure 9 shows the temperature dependence of the electrical resistivity for CeRuSn$_x$ ($2.85 \leqslant x \leqslant 3.15$). In the Sn excessive case, the resistivity becomes smaller with increasing x. The temperature dependence of the resistivity for $x = 3.03$ and 3.09 is not much different from the stoichiometric sample, while the excess of 5 at.% of Sn ($x = 3.15$) leads to drastic decrease of the resistivity at low temperature. In this sample, the extraction of pure Sn was confirmed by x-ray diffraction measurement and the gradual decrease of the resistivity below 3.7 K is due to the superconducting transition of the extracted Sn. The temperature dependence of the resistivity for the Sn deficient samples shows three step anomalies. The absolute value of the resistivity decreases with decreasing x. For $CeRuSn_{2.91}$, we observe drastic decreases of resistivity at 33 K, 4 K and 1.3 K. According to Takayanagi [20], the low temperature specific heat of $CeRuSn_{2.91}$ shows a clear lambda-type anomaly around 1.3 K, indicating some kind of phase transition at this temperature.

Figure 10 shows the temperature dependence of TEP for CeRuSn$_x$ ($2.85 \leqslant x \leqslant 3.15$). The TEP of CeRuSn$_x$ are very sensitive to the Sn content. The excess of Sn leads to

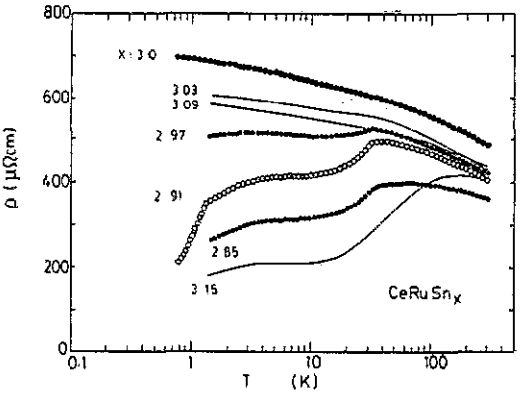

Figure 9. Temperature dependence of the electrical resistivity for $CeRuSn_x$ ($2.85 \leq x \leq 3.15$).

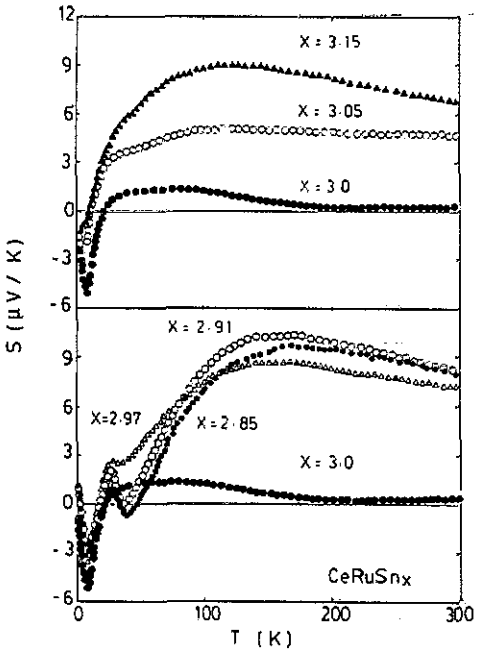

Figure 10. Temperature dependence of the thermoelectric power (TEP) for $CeRuSn_x$ ($2.85 \leq x \leq 3.15$).

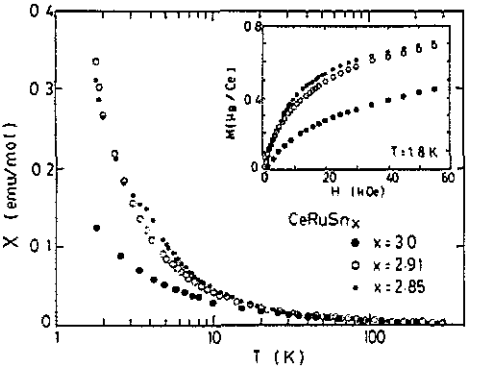

Figure 11. Temperature dependence of the magnetic susceptibility for $CeRuSn_x$ ($x = 2.85$, 2.91 and 3.0). The inset shows the magnetization as a function of the magnetic field at 1.8 K.

increase of TEP and gradual disappearance of a negative peak around 8 K. The deficiency of Sn leads to drastic increase of TEP at high temperatures. At lower temperatures (<50 K), TEP of the Sn deficient sample has a negative peak around 8 K and a positive peak around 28 K which gradually grow with decreasing x. These TEP peaks correlate with the drastic decreases of the resistivity. The sign of TEP at 1.6 K changes from negative to positive with decreasing Sn content. The TEP of the stoichiometric compound approaches zero with decreasing temperature after passing through the negative peak.

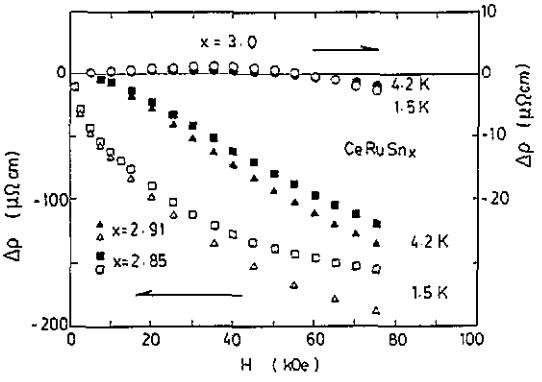

Figure 12. Field dependence of the longitudinal magnetoresistivities (LMR) for $CeRuSn_x$ ($x = 2.85$, 2.91 and 3.0) at 4.2 K and 1.5 K.

For $x = 2.91$ and $x = 2.85$, TEP changes sign from negative to positive near 3 K, below which we expect a positive peak, possibly related to the magnetic transition at 1.3 K.

As to x dependence of the low temperature resistivity, a maximum was observed at $x = 0$. In the same way, the high temperature TEP have a minimum at $x = 0$. These facts suggest that the absence of the coherence effect in $CeRuSn_3$ is not due to deviation from stoichiometry.

In order to know the magnetic properties of Sn deficient Ce compounds, magnetic susceptibility, magnetization, Hall coefficient and high field Hall resistivity and magnetoresistivity have been investigated on $CeRuSn_x$ ($x = 2.91$ and 2.85).

Figure 11 shows the temperature dependence of the magnetic susceptibility for $CeRuSn_x$ ($x = 3.0$, 2.91 and 2.85). The susceptibility follows the Curie–Weiss law between 100 K and 300 K with the paramagnetic Curie temperatures of −66 K, −38 K and −34 K for $x = 3.0$, 2.91 and 2.85. The susceptibility of the Sn deficient samples is gradually enhanced below 50 K. There is no anomaly near 30 K corresponding to those observed in the resistivity and TEP. The susceptibility of $CeRuSn_{2.91}$ increases smoothly down to 1.8 K, while the susceptibility for $CeRuSn_{2.85}$ shows a small bump around 4 K. At the present stage, it is not clear whether this bump is intrinsic or not.

The inset of figure 11 shows the field dependence of magnetization at 1.8 K. The magnetization of the Sn deficient samples is enhanced compared to the stoichiometric sample. The magnetization of the Sn deficient samples at 55 kOe reaches $0.7\mu_B$/Ce atom which is close to the full moment of a Γ_7-doublet $0.71\mu_B$. The magnetization of $CeRuSn_{2.85}$ shows metamagnetic-like behaviour around 6 kOe below 4 K. This metamagnetic transition is related to the bump of susceptibility at 4 K.

Figure 12 shows the field dependence of the longitudinal magnetoresistivity (LMR) for $CeRuSn_x$ ($x = 3.0$, 2.91 and 2.85) at 4.2 K and 1.5 K. The LMR of $CeRuSn_3$ is very small and shows an anomalous positive contribution at low fields. This behaviour is possibly explained by the competition between a negative contribution from the Kondo effect and a positive one from the localization effect. The LMR of the Sn deficient samples shows large negative values. In particular, the LMR of $CeRuSn_{2.91}$ at 1.5 K amounts to about $-200\ \mu\Omega$ cm comparable with the temperature dependent resistivity decrease below the magnetic ordering temperature 1.3 K (figure 9). The applied magnetic field assists the ordering of magnetic moments just above the transition temperature.

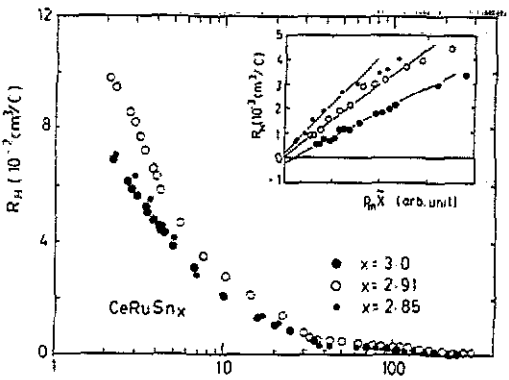

Figure 13. Temperature dependence of the Hall coefficient for $CeRuSn_x$ ($x = 2.85, 2.91$ and 3.0). The inset shows the Hall coefficient as a function of $\rho_m \cdot \tilde{\chi}$ where ρ_m is the magnetic resistivity and $\tilde{\chi}$ is the normalized susceptibility.

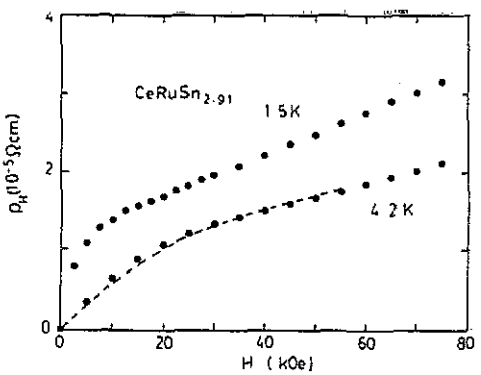

Figure 14. Field dependence of the Hall resistivity for $CeRuSn_{2.91}$ at 4.2 K and 1.5 K. The broken curve shows the best fitted curve to equation (5) at 4.2 K.

Figure 13 shows the temperature dependence of the Hall coefficient for $CeRuSn_x$ ($x = 3.0, 2.91$ and 2.85). The Hall coefficient of the Sn deficient samples shows monotonic increase down to 2 K with decreasing temperature. These is no anomaly near 30 K where the resistivity shows drastic decrease and the TEP shows a maximum. No Hall coefficient maximum, which is characteristic of the coherent state of heavy fermion compounds, has been observed at least down to 2 K. This means that the resistivity decrease of the Sn deficient samples near 30 K is not due to the coherence effect. As shown in figure 6, the Hall coefficient of the stoichiometric sample can be fitted well to the expression due to skew scattering by independent Ce impurities. From equation (3), we can estimate R_0 using a $\rho_m\tilde{\chi}$ against R_H plot. The inset of figure 13 shows $\rho_m\tilde{\chi}$ versus R_H plots for the three compounds. R_H of the stoichiometric sample shows clear linear $\rho_m\tilde{\chi}$ dependence. R_H of the Sn deficient samples depends linearly on $\rho_m\tilde{\chi}$ above 100 K. We estimated R_0 for these compounds using least square fitting to equation (3). The estimated R_0 are -2, -0.3 and 2 ($\times 10^{-4}$ cm^3/C) for $x = 3.0$, 2.91 and 2.85, respectively. This successive increase of R_0 with decreasing x suggests that the Sn deficiency induces a change in carrier concentration.

Figure 14 shows the field dependence of the Hall resistivity ρ_H for $CeRuSn_{2.91}$ up to 75 kOe at both 4.2 K and 1.5 K. The anomalous part of the Hall coefficient becomes

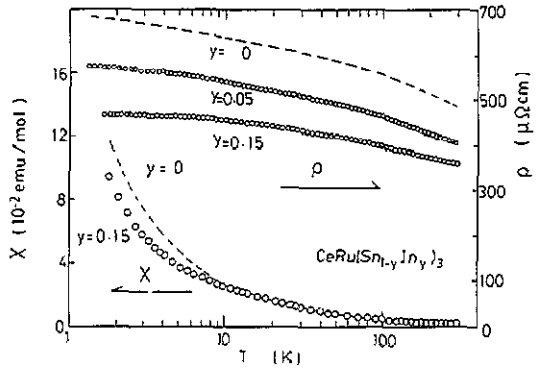

Figure 15. Temperature dependence of electrical resistivity and magnetic susceptibility for $CeRu(Sn_{1-y}In_y)_3$ ($y = 0.15$ and 0.05).

larger with decreasing temperature. In the figure, the broken curve shows the best fit curve at 4.2 K to a conventional expression for the Hall resistivity in magnetic materials

$$\rho_H = R_0 H + R_A M \tag{4}$$

where R_A is the anomalous Hall coefficient and M is the magnetization. In equation (4), we first assumed that R_A is not dependent on the field. R_0 was adjusted to get the best fit to equation (4). We obtained $R_0 = -7 \times 10^{-4}$ (cm^3/C) from this fitting. The normal Hall resistivity thus estimated is less than 10% at 10 kOe of the measured Hall resistivity, suggesting the dominance of the anomalous Hall part. R_0 values thus determined one more than an order of magnitude smaller compared to the high temperature limit value -0.3×10^{-4} (cm^3/C) determined from the plot in figure 13. We cannot, however, rule out the possibility of the field dependence of R_A.

In order to clarify the effect of carrier concentration change in $CeRuSn_x$, we have prepared $CeRu(Sn_yIn_{1-y})_3$ ($y = 0.05$ and 0.15). Figure 15 shows the temperature dependence of electrical resistivity and magnetic susceptibility for $CeRu(Sn_yIn_{1-y})_3$ ($y = 0$, 0.05 and 0.15). The resistivity shows successive decrease with increasing y. As to the effect on the carrier concentration, we expect that the 15 at.% substitution of In for Sn gives the same contribution as 5 at.% Sn deficiency. The room temperature resistivities for $CeRuSn_{2.85}$ and $CeRu(Sn_{0.85}In_{0.15})_3$ have the same value 360 ± 40 $\mu\Omega$ cm within the experimental error as expected. The temperature dependence of the resistivity of $CeRu(Sn_yIn_{1-y})_3$ ($y = 0.05$ and 0.15) is monotonic, however, and any anomalies which were observed in the Sn deficient samples have not been observed. In contrast with the enhanced susceptibility of the Sn deficient samples, the magnetic susceptibility of the In alloy is reduced compared to the stoichiometric sample. These facts imply that some additional effects other than carrier concentration change play a very important role in the Sn deficient samples.

In order to know the effect of the Sn deficiency on a non-Kondo system, we have prepared $NdRuSn_{2.91}$. Figure 16 shows the temperature dependence of the magnetic susceptibility and the electrical resistivity for $NdRuSn_x$ ($x = 3.0$ and 2.91). The susceptibility of $NdRuSn_{2.91}$ obeys the Curie–Weiss law between 30 K and 300 K with an effective moment of 3.6 μ_B/Nd and a paramagnetic Curie temperature of -13 K. An

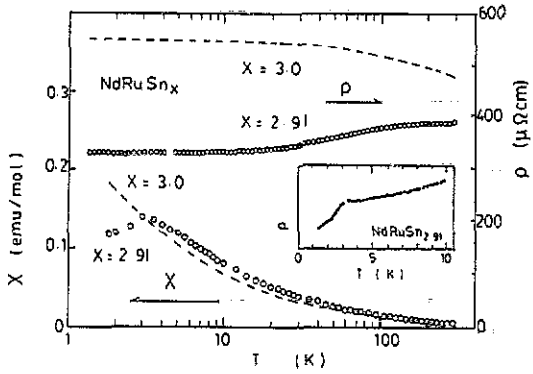

Figure 16. Temperature dependence of electrical resistivity and magnetic susceptibility for $NdRuSn_x$ ($x = 2.91$ and 3.0). The inset shows an enlarged view of the electrical resistivity of $NdRuSn_{2.91}$ near $T_N = 6$ K.

obvious cusp-like peak of susceptibility was observed at 3 K, suggesting an antiferromagnetic transition. Both in $CeRuSn_3$ and $NdRuSn_3$ systems, Sn deficiency induces magnetic transitions and simultaneously leads to the resistivity decrease. These facts suggest that the low magnetic phase transition temperature (possibly the absence of a magnetic transition) has some correlation with the large residual resistivities in these compounds.

4. Summary

The experimental results on $RERuSn_3$ (Re = La, Ce, Pr, Nd and Sm) and $CeRuSn_x$ ($2.85 \leqslant x \leqslant 3.15$) are summarized as follows.

(1) The susceptibility of $RERuSn_3$ (RE = Ce, Pr and Nd) indicates no sign of magnetic ordering down to 1.8 K. For $CeRuSn_3$, we have not observed the Kondo coherence effect. The electrical resistivity and the Hall coefficient follow the dilute Kondo theorem between 2 K and 300 K.

(2) The lattice constant and the magnetic susceptibility measurements indicate that $SmRuSn_3$ is a new valence fluctuating compound. The valency of Sm ions which is estimated from the susceptibility measurement is about 2.8. $SmRuSn_3$ shows an antiferromagnetic transition at 6 K. The temperature dependence of the resistivity also suggests the formation of an antiferromagnetic gap below 6 K.

(3) The electrical resistivity results and TEP for $CeRuSn_x$ ($2.85 \leqslant x \leqslant 3.15$) imply that the absence of coherency in $CeRuSn_3$ is not due to deviation from stoichiometry.

(4) The Sn deficiency in $CeRuSn_x$ ($x \leqslant 3$) induces some phase transitions at 33 K, 4 K and 1.3 K. In these transitions, 1.3 K is the magnetic ordering temperature. The Sn deficiency induces magnetic ordering also in the localized magnetic moment system $NdRuSn_{2.91}$. The Hall coefficient measurement on $CeRuSn_x$ ($x = 2.85$, 2.91 and 3) reveals that the Sn deficiency induces the change of the carrier concentration. The appearance of the phase transitions in the Sn deficient samples cannot, however, be attributed only to the change in the carrier concentration, since the In alloys do not show any phase transition.

Acknowledgments

The authors are grateful to Professors S Takayanagi, Y Onuki, T Komatsubara, K Yonemitsu and I Shiozaki for their helpful discussion. This work was partly supported by the priority area project on the physics of actinide compounds, a Grant-in-Aid for Scientific Research from the Ministry of Education, Science and Culture.

References

[1] Onuki Y, Komatsubara T 1987 *J. Magn. Magn. Mater.* **63–64** 281
[2] Andres K, Graebner J E and Ott H R 1975 *Phys. Rev. Lett.* **35** 1779
[3] Andres K and Baucher 1978 *J. Low Temp. Phys.* **9** 268
[4] Matthias B T, Gebelle T H, Andres K, Corenzit E, Hull G W and Matia J P 1968 *Science* **159** 530
[5] Onuki Y, Ina K, Nisihara M, Komatsubara T, Takayanagi S, Kameda K and Wada N 1986 *J. Phys. Soc. Japan* **55** 1818
[6] Kasaya M, Liu B, Sera M, Kasuya T, Goto T and Fujimura T 1985 *J. Magn. Magn. Mater.* **52** 289
[7] Eisenmann B and Schäfer H 1986 *J. Less-Common Met.* **123** 89
[8] Remeika J P, Espinosa G P, Cooper A S, Barz H, Rowell J M, McWhan D B, Vandenberg J M, Monton D E, Fisk Z, Woolf L D, Hamaker H C, Maple M B, Shirane G and Thomlinson W 1980 *Solid State Commun.* **34** 923
[9] Fukuhara T, Sakamoto I, Sato H, Takayanagi S and Wada N 1989 *J. Phys.: Condens. Matter* **1** 7487
[10] Menovsky A and Franse J J 1983 *J. Cryst. Growth* **65** 286
[11] Takayanagi S, Fukuhara T, Sato H, Wada N and Yamada Y 1991 *Physica* B **165 & 166** 447
[12] Kasaya M, Tarascon J M and Etournean J 1980 *Solid State Commun.* **33** 1005
[13] Kasaya M and Iga Y 1986 *AIP Conf. Proc.* **140** 11
[14] Vodop'yanov B P, Garifullin I A and Garif'yanov N N 1987 *JETP Lett.* **46** 95
[15] Najib A, Pierre J, Besnus M J, Harn P, Murani A P and Siaud E 1988 *Z. Phys.* B **73** 49
[16] Souletie J 1975 *J. Phys. F: Met. Phys.* **5** 329
[17] Fert A, Hamzic A and Levy P M 1987 *J. Magn. Magn. Mater.* **63 & 64** 535
[18] Takayama H and Fulde P 1975 *Z. Phys.* B **20** 81
[19] Jaccard D and Sierro J 1982 *Valence Instabilities* ed Wacher P and Boppart H (Amsterdam: North-Holland) p 459
[20] Takayanagi S 1991 private communication